Reprinted from SPINE, Vol. 22, No. 21, November 1, 1997

Printed in the U.S.A.

Analysis of Symmetry of Vertebral Body Loading Consequent to Lateral Spinal Curvature

Ian A. F. Stokes, PhD

Study Design. A biomechanical model was used to calculate muscle and intervertebral forces in a spine with and without a lumbar scoliosis.

Objectives. To quantify the loading of the motion segments in a lumbar scoliosis.

Summary of Background Information. Scoliosis is thought to cause asymmetric loading of vertebral physes, causing asymmetric growth according to the Hueter–Volkmann principle. The magnitude of vertebral loading asymmetry as a function of scoliosis magnitude is unknown, however, as is the sensitivity of growth to asymmetric loading.

Methods. The analysis included five lumbar vertebrae, the thorax, and the sacrum/pelvis and 90 pairs of multijoint muscles. Five spinal geometries were analyzed: the mean spinal shape of 15 patients with left lumbar scoliosis (38° Cobb angle, apex at L1–L2, the reference or "100%" geometry), and the geometry scaled to 0%, 33%, 67%, and 132% of the asymmetry of the reference shape. The muscle and intervertebral forces for maximum efforts opposing moments applied to the T12 vertebra in each of the three principal directions were calculated. The loading at each intervertebral level was expressed as the resultant force (P), the axial torque, the lateral and anteroposterior offset of P from the disc center, and the angle of P from the axial direction.

Results. With increasing scoliosis, there was a weak trend of increasing lateral offset of P, but not consistently to either the convex or concave direction. There was a much stronger trend of increasing angle between the force P and the motion segment longitudinal axis with increasing Cobb angle. Typically, this angle was 10–30° for the largest scoliosis (51° Cobb) and in a direction tending to increase the scoliosis. This angulation of the force results from shear loading of the disc. Axial torques tending to increase the transverse plane deformity increased with scoliosis for extension efforts.

Conclusions. These analyses indicate that lumbar scoliosis produces asymmetric spinal loading characterized by shear forces tending to increase the scoliosis, but with little increase in the asymmetric compression of motion segments. If scoliosis progression results from asymmetric loading, it appears that the shear force component is responsible. [Key words: biomechanical model, lumbar spine, progressive deformity, scoliosis] **Spine 1997;22:2495–2503**

From the Department of Orthopaedics and Rehabilitation, University of Vermont, Burlington, Vermont.
Supported by an NIH award R01 HD 31167, Fogarty International Center award F06 TW 01948-01 and the Scoliosis Research Society 1993/4 Research Award.
Part of this work was done while IAFS was Professeur Invité at the École Nationale Supérieure d'Arts et Métiers, Paris.
Acknowledgment date: August 21, 1995.
First revision date: February 15, 1996.
Acceptance date: May 31, 1996.
Device status category: 1.

The progression of spinal deformity is thought to be primarily biomechanical. According to this thesis, lateral curvature alters the spinal and muscular geometry and muscle activation patterns and causes asymmetric loading of vertebrae.[1,9] This asymmetric loading, in turn, is thought to promote asymmetric growth of the spine and progression of deformity. The adolescent growth spurt is the danger period for progression of both neuromuscular and idiopathic scoliosis, although larger curves continue to progress even after skeletal maturity.[2,6,14] The mechanical modulation of growth in physes often is referred to as the "Hueter–Volkmann Law."[5,10,12,13]

In treating spinal deformity, mechanical forces from braces are used to modify the development of spinal shape. The scientific basis for conservative treatment thus is handicapped by the lack of understanding of the pathomechanics of scoliosis progression. It has never clearly been established whether or not young patients with scoliosis should participate in sports and other activities that might asymmetrically stress their spine and promote progression of the deformity.

The magnitude of the asymmetry of loading of vertebrae in scoliosis has not been measured directly and depends on the magnitude of muscle forces. Rueber[9] and Zetterberg[15] both reported asymmetries of the electromyographic recordings of the dorsal muscles of patients with scoliosis; they thought that this was due to secondary changes in the moments of the muscles about the spine. Miller and Skogland[7] developed a three-dimensional model of the thoracic and lumbar spine and reported the muscle forces and spine loading associated with maintenance of posture under the influence of gravity loads, with idealized lateral deformities of vertebrae to represent scoliosis. When the induced asymmetry consisted of a 5-mm lateral displacement of a vertebra, the calculations showed that the lateral bending moment

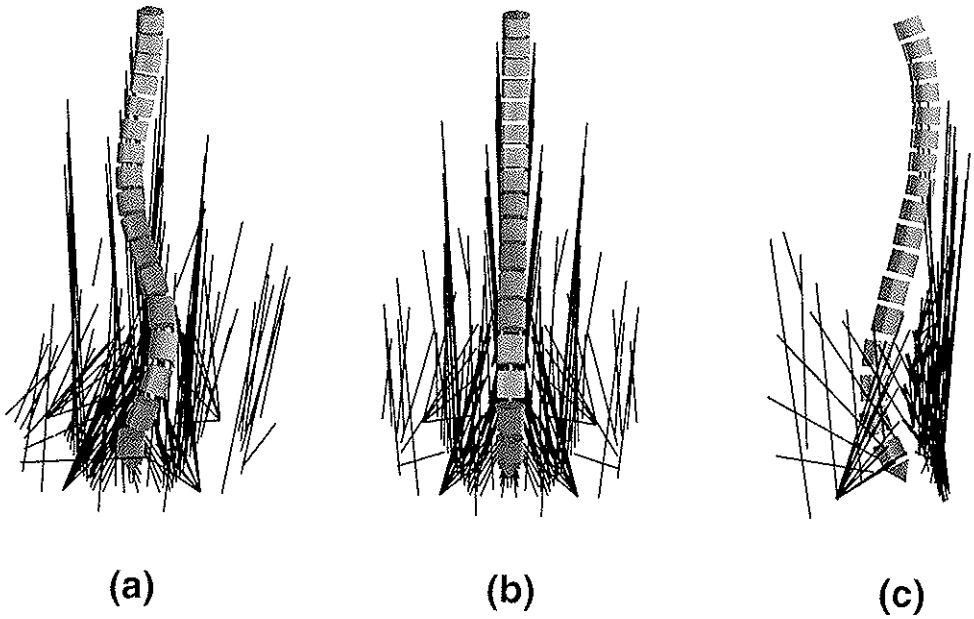

Figure 1. Spinal shape used to represent **(a)** the spine with scoliosis and **(b and c)** the symmetric spine. Parts **a** and **b** are anteroposterior views; **c** is a lateral view. Each cylinder represents the position of a vertebra. The straight lines represent the paths of 90 pairs of muscles that cross the lumbar spine. Because many of these muscles insert into the thoracic spine, the thoracic geometry was important to this analysis of lumbar spine loading.

was on the order of 1 Nm, with the compressive load being approximately 100 N. This combination of axial load and lateral bending moment corresponds to a 10-mm lateral displacement of the resultant force from the disc center.

There is very little quantitative information about how scoliosis affects the loads acting on the spine and on the sensitivity of growth to asymmetric loading. In this study, the author addresses the first of these unknowns using a biomechanical analysis of the forces in the muscles and the degree of asymmetric loading of a spine with lateral curvature (scoliosis). Ultimately, combining a knowledge of spinal loading asymmetry and of the sensitivity of spinal growth to load would allow one to quantify how mechanical factors determine scoliosis progression during growth.

The purpose of this study was to obtain quantitative estimates of the degree of vertebral asymmetric loading in the lumbar spine with scoliosis for maximum efforts in flexion, extension, lateral bending, and axial rotation and to compare these with the corresponding values for a spine that is symmetric about the sagittal plane.

■ Methods

The analysis was based on an analytical model of muscular forces in the lumbar spine reported by Stokes and Gardner-Morse.[11] The model includes five lumbar vertebrae, six intervertebral motion segments, the thoracic spine, and the sacrum/pelvis, to which are attached 90 pairs of multijoint muscles.

The spinal and muscle geometry was modified into four shapes representing a graded increase in scoliosis: 0%, 33%, 67%, 100%, and 132% of a reference deformity. The reference deformity (100%) was averaged from stereo-radiographic measurements of the thoracic and lumbar spinal shape of 15 patients with left lumbar scoliosis (mean Cobb angle, 38°; range, 27–43°; mean age, 16 years). The apex was at L1–L2 (Figure 1a). To produce the 0% scoliosis geometry, the spine was made symmetric about the sagittal plane by eliminating any lateral deviation and axial rotation of the vertebrae (Figures 1b and 1c). Then two additional geometries (33% and 67%) were interpolated between the 0% and the 100% cases, and one geometry (132%) was extrapolated from it. The Cobb angles of the resulting curves were 0°, 13°, 26°, 38°, and 51°.

The model used published anatomic data for the muscle insertions and muscle maximum contractile force. Data for the

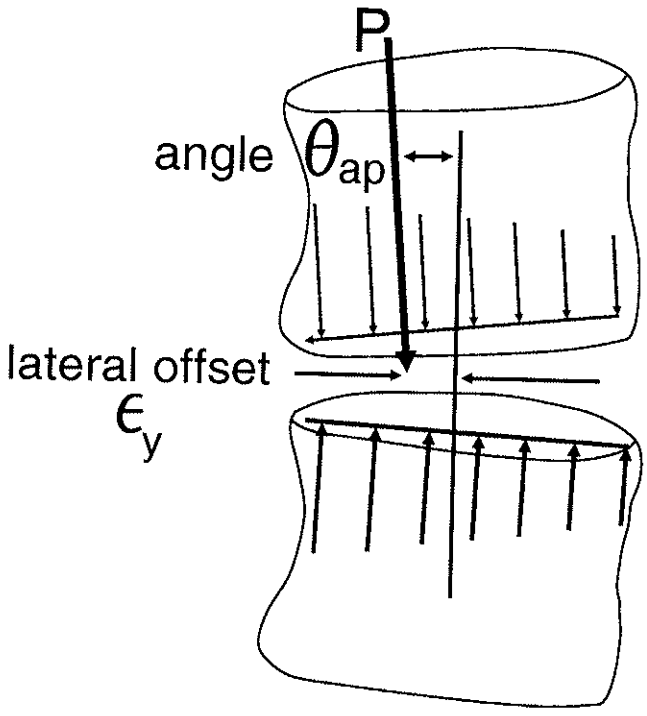

Figure 2. Assumed asymmetry of loading of vertebral growth plates in a scoliosis deformity, quantified by lateral load offset ϵ_y from the disc center and as the angle Θ_{ap} of the resultant force from the plane of the intervertebral disc.

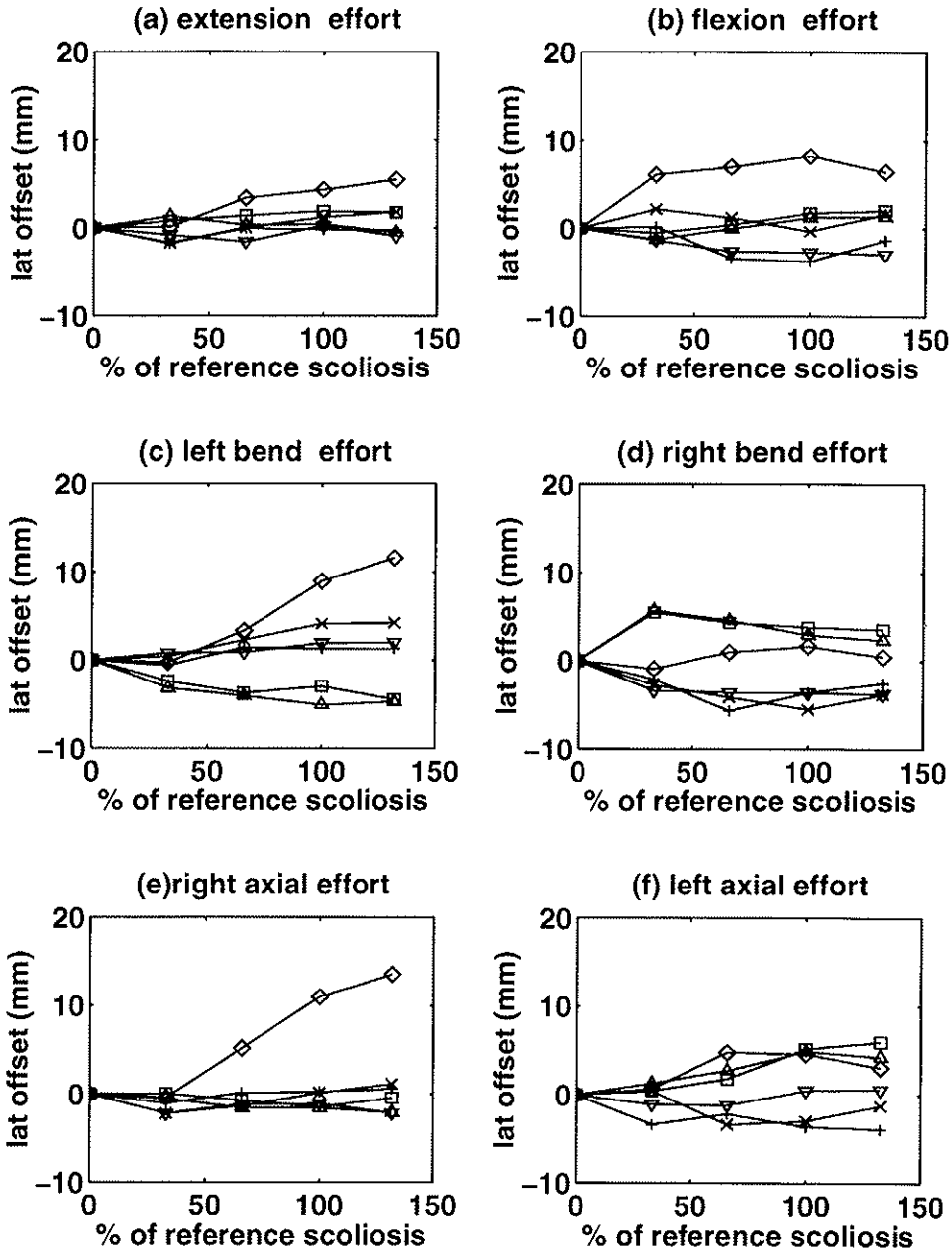

Figure 3. The lateral offset of the intervertebral force ϵ_Y as a function of model geometry (percent of reference geometry). The values plotted are differences from the values for the 0° (reference) geometry, which are given in Table 1. **a,** maximum extension efforts; **b,** maximum flexion efforts; **c,** maximum left lateral bending efforts; **d,** maximum right lateral bending efforts; **e,** maximum right axial rotation efforts; and **f,** maximum left axial rotation efforts.

dorsal muscles and the psoas were obtained from published data expressing the muscle anatomy descriptively in terms of locations of attachments to the vertebrae and quantitatively by the physiologic cross-sectional area as described by Stokes and Gardner-Morse.[11] The quadratus lumborum muscles were added using data from Han et al.[4] The oblique abdominal muscles and rectus abdominus were obtained from averaged digitized outlines of serial magnetic resonance image scans of 15 healthy male volunteers. Volumetric reconstructions of these outlines were expressed as an equivalent line of action for each side of the rectus abdominus and as six equivalent lines for each of the internal and external oblique muscles. The lines of action were based on the predominant fiber directions visible in anatomic specimens. The only significant missing muscles were the transversus abdominis and latissimus dorsi. Finally, the muscle attachments were referred to the coordinate system defining the bony anatomy of each of the four skeletal geometries.

The lumbar spinal motion segments were represented in the analyses by flexible beam elements with stiffness as derived by Gardner-Morse et al[3] from data of Panjabi et al[8] for adult thoracic spines. The sensitivity of the results to the motion segment stiffness was assessed by repeating some of the analyses with stiffness reduced by a factor of two because Miller and Skogland[7] measured the flexibility of motion segments of an adolescent human and reported flexibilities for the thoracic region approximately twice as high as those of Panjabi et al.[8]

The model was used to calculate the lumbar spinal loads corresponding to maximum efforts in the three principal moment directions at the T12 vertebra. This analysis was restricted to maximum efforts because at submaximal efforts there is a highly redundant set of permutations of muscle re-

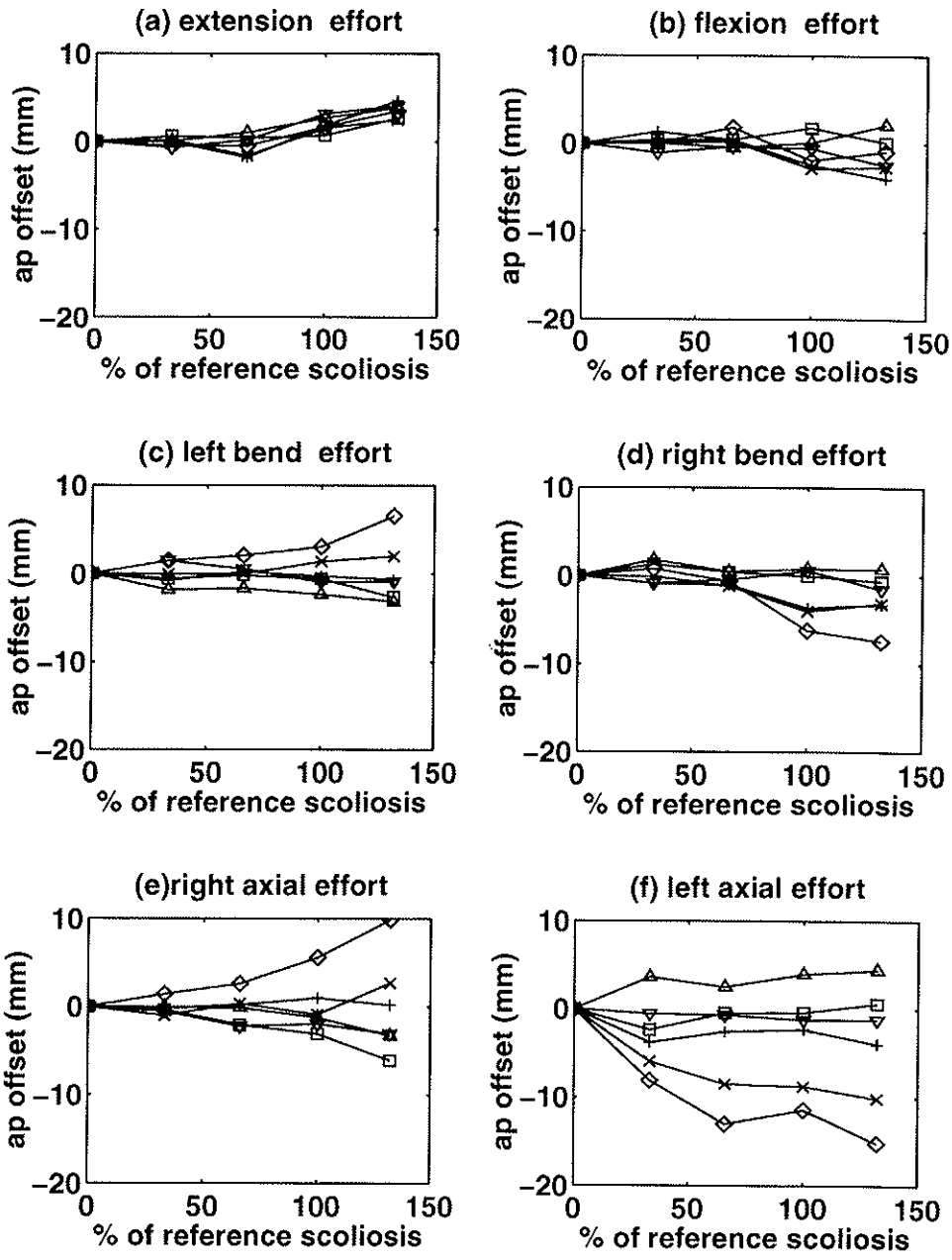

Figure 4. The anteroposterior offset of the intervertebral force ϵ_x as a function of model geometry (percent of reference geometry). The values plotted are differences from the values for the 0° (reference) geometry, which are given in Table 1. **a**, maximum extension efforts; **b**, maximum flexion efforts; **c**, maximum left lateral bending efforts; **d**, maximum right lateral bending efforts; **e**, maximum right axial rotation efforts; and **f**, maximum left axial rotation efforts.

cruitments that can oppose a given set of external forces. As discussed in Stokes and Gardner-Morse[11], the solution for the muscle recruitment strategy to produce maximal voluntary effort usually can be found with a unique solution not requiring the imposition of a physiologic cost function. This solution was obtained by solving a linear program (using the lp solve routine, author Michel Berkelaar <michel@es.ele.tue.nl>, obtained by anonymous ftp from ftp.es.ele.tue.nl in directory pub/lp_solve). The objective was to calculate the maximum efforts, subject to constraints of equilibrium, with muscle forces constrained to be non-negative and less than a physiologic maximum proportional to their cross-sectional area (460 kPa) and with physiologic limits imposed on motion segment elastic displacements (5 mm and 5° in the sagittal plane and 2 mm and 2° in the other planes).[11]

The intervertebral forces then were calculated relative to the local axes (x, y, z) of each motion segment. In this local axis system, z was the line joining the centers of adjacent vertebrae (positive cephalad), x lay in the local sagittal plane of the motion segment (positive forward), and y was perpendicular to x and z (positive to the left). The loading state of each motion segment was expressed as a lateral offset from the disc center and as the angle of the resultant force from the frontal plane of the motion segment (Figure 2). Five measures of the loads transmitted by the motion segments, P, T_z, ϵ_y, ϵ_x and Θ_{ap}, were considered.

P = the total (resultant) intervertebral force.

T_z = the axial torque transmitted through the motion segment.

ϵ_y = lateral offset of the intervertebral force P from the disc center.

ϵ_x = offset of the intervertebral force P from the disc center in the sagittal plane.

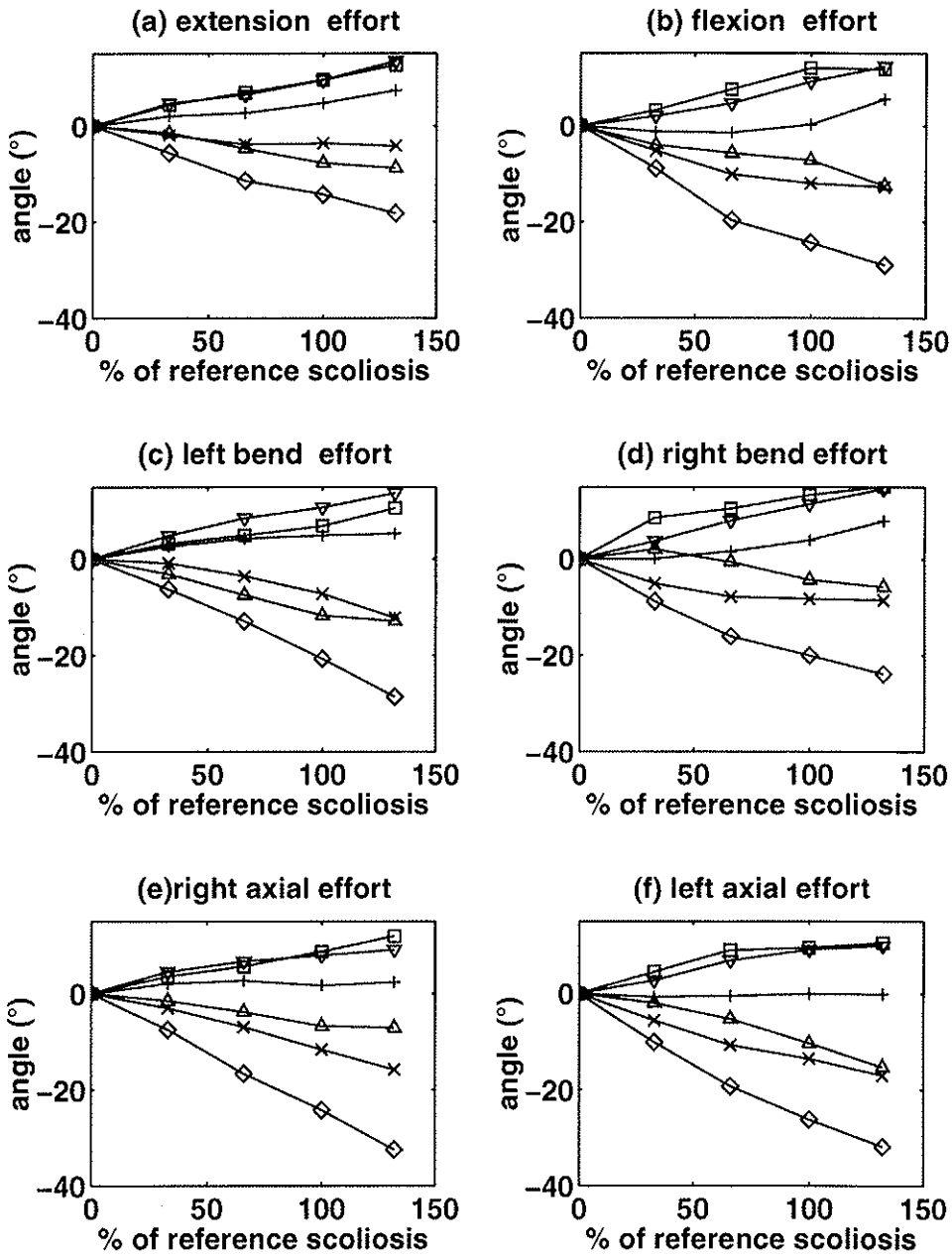

Figure 5. The angulation Θ_{ap} of the intervertebral force as a function of model geometry (percent of reference geometry). The values plotted are differences from the values for the 0° (reference) geometry, which are given in Table 1. **a,** maximum extension efforts; **b,** maximum flexion efforts; **c,** maximum left lateral bending efforts; **d,** maximum right lateral bending efforts; **e,** maximum right axial rotation efforts; and **f,** maximum left axial rotation efforts.

Θ_{ap} = the angle in the frontal plane of P to the intervertebral axis.

The derived measures were calculated as follows:

$$\epsilon_y = M_x/P_z;\ \epsilon_x = M_y/P_z \quad (1 \text{ and } 2)$$

$$\Theta_{ap} = \text{atan}(P_y/P_z) \quad (3)$$

where:

M_x = the lateral bending moment transmitted through the motion segment.

M_y = the flexion–extension bending moment transmitted through the motion segment.

P_y = the lateral shear component of the intervertebral force.

P_z = the axial component of the intervertebral force.

The lateral offset ϵ_y is therefore a measure of the lateral bending moment M_x transmitted through the motion segment, the anteroposterior offset ϵ_x is a measure of the flexion/extension moment M_y, and the angulation Θ_{ap} of the resultant force P is a measure of the lateral shear force acting on the motion segment.

■ Results

There was a weak trend of increasing lateral offset of the resultant intervertebral force with increasing scoliosis, but not consistently to either the convex or concave direction (Figures 3a–3f). Similarly, there was no consistent trend for the anteroposterior offset (Figure 4). A much stronger trend was evident for the angle of the resultant force to the axial direction, which was typically at 10–30° to the local axial direction for the largest scoliosis considered (51° Cobb; see Figures 5a–5f). This angulation of the resultant force corresponded to interver-

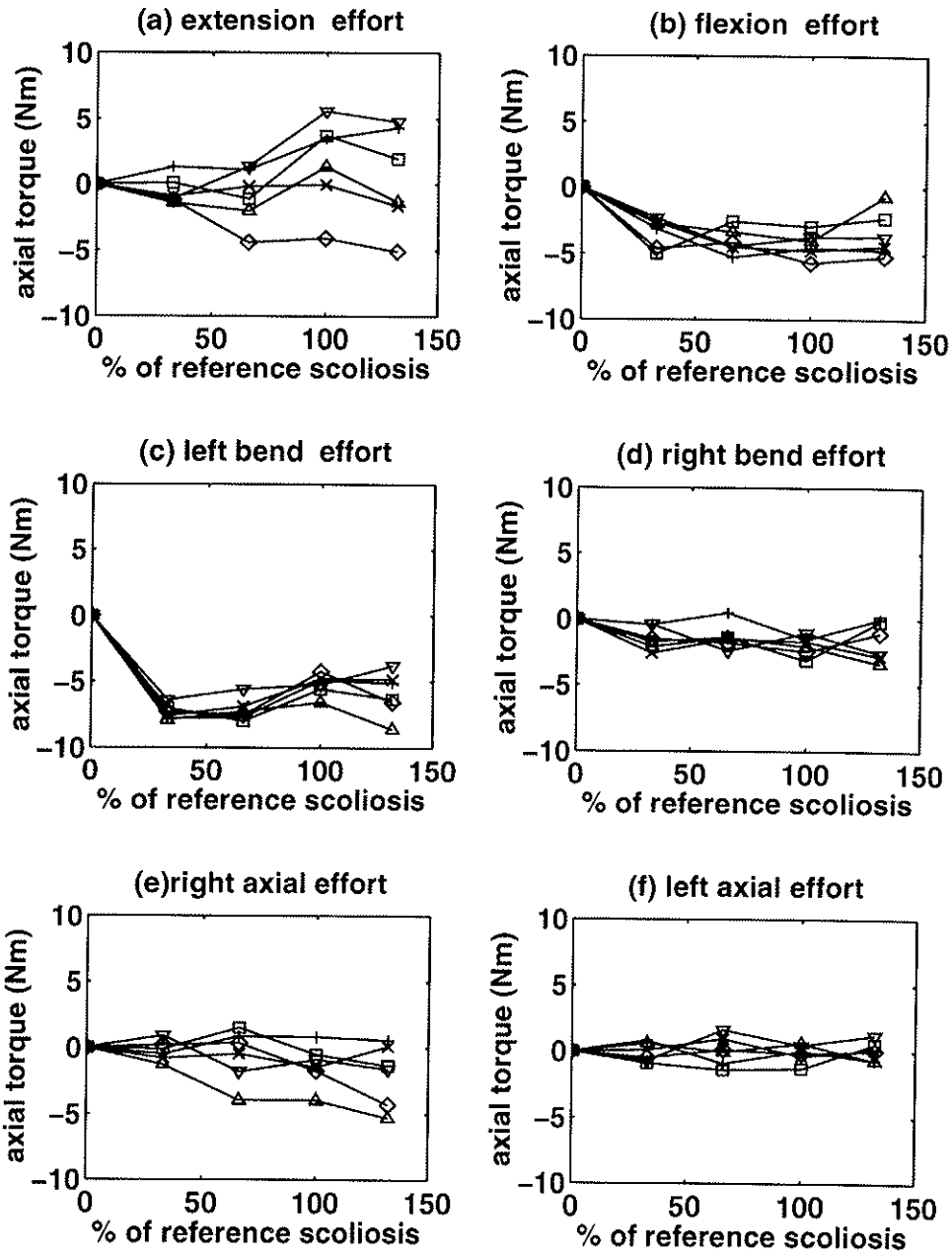

Figure 6. The intervertebral axial torque T_z as a function of model geometry (percent of reference geometry). The values plotted are differences from the values for the 0° (reference) geometry, which are given in Table 1. **a**, maximum extension efforts; **b**, maximum flexion efforts; **c**, maximum left lateral bending efforts; **d**, maximum right lateral bending efforts; **e**, maximum right axial rotation efforts; and **f**, maximum left axial rotation efforts.

tebral shear forces tending to increase the scoliosis, because a positive value indicated intervertebral forces tending to displace the upper vertebra to the left relative to the lower one. In Figure 6, there is no clear trend of axial torque changes with increasing scoliosis except for extension efforts (Figure 6a), where the torque is predominantly positive below the apex and negative above it. This pattern of torques would tend to increase the transverse plane vertebral rotations. Figures 3–6 present the differences between the values of the force asymmetry measures ϵ_y, ϵ_x, Θ_{ap}, and T_z and the corresponding values for the 0% scoliosis case. The values for the 0% scoliosis case are given in Table 1. The values in Table 1 should be added to any values shown in Figures 3–6 to obtain the real values for any case.

In Figures 3–6, the sign conventions are as follows: Extension effort (Figures 3a, 4a, 5a, and 6a) simulated a subject attempting to extend the trunk against a resistance; left lateral bend (Figures 3c, 4c, 5c, and 6c) was an attempt to bend the trunk to the left against resistance, and right axial effort (Figures 3e, 4e, 5e, and 6e) meant a subject attempts to rotate the trunk to the right against a resistance. A positive value of the lateral force offset ϵ_y indicates a displacement of the resultant intervertebral force to the left, and a positive value of the anteroposterior offset ϵ_x indicates a forward displacement of the resultant force. A positive value of the angulation Θ_{ap} indicates that there is a force tending to displace the upper vertebra of a motion segment to the left, relative to the lower vertebra. Therefore, the results in Figures

Table 1. Intervertebral Loading Asymmetry at Each Level of the 0% Scoliosis (Symmetrical) Model

	Extension Effort	Flexion Effort	Left Lateral Effort	Right Lateral Effort	Right Axial Effort	Left Axial Effort
T12–L1 lat offset (mm)	0.0	0.0	−3.8	3.8	−4.7	4.7
T12–L1 ap offset (mm)	8.4	12.6	8.8	8.8	11.1	−11.1
T12–L1 angle (°)	0.0	0.0	−1.0	1.0	2.3	−2.3
T12–L1 Torque (Nm)	0.0	0.0	2.7	−2.7	5.0	−5.0
L1–L2 lat offset (mm)	0.0	0.0	−3.8	3.8	−1.1	1.1
L1–L2 ap offset (mm)	4.3	4.3	1.0	1.0	1.1	1.1
L1–L2 angle (°)	0.0	0.0	−0.4	0.4	3.3	−3.3
L1–L2 Torque (Nm)	0.0	0.0	3.2	−3.2	5.8	−5.8
L2–L3 lat offset (mm)	0.0	0.0	−1.3	1.3	1.9	−1.9
L2–L3 ap offset (mm)	0.0	−3.7	−2.1	−2.1	−4.3	−4.3
L2–L3 angle (°)	0.0	0.0	0.7	−0.7	3.4	−3.4
L2–L3 Torque (Nm)	0.0	0.0	4.4	−4.4	4.7	−4.7
L3–L4 lat offset (mm)	0.0	0.0	−2.1	2.1	3.7	−3.7
L3–L4 ap offset (mm)	−4.5	−4.9	−3.3	−3.3	−4.4	−4.4
L3–L4 angle (°)	0.0	0.0	0.8	−0.8	2.6	−2.6
L3–L4 Torque (Nm)	0.0	0.0	3.2	−3.2	5.6	−5.6
L4–L5 lat offset (mm)	0.0	0.0	3.3	−3.3	2.3	−2.3
L4–L5 ap offset (mm)	−3.5	−2.6	−1.1	−1.1	0.0	0.0
L4–L5 angle (°)	0.0	0.0	3.0	−3.0	−0.2	0.2
L4–L5 Torque (Nm)	0.0	0.0	2.8	−2.8	3.5	−3.5
L5–S1 lat offset (mm)	0.0	0.0	3.6	−3.6	2.1	−2.1
L5–S1 ap offset (mm)	3.0	6.9	5.6	5.6	5.6	5.6
L5–S1 angle (°)	0.0	0.0	3.8	−3.8	−2.2	2.2
L5–S1 torque (Nm)	0.0	0.0	2.6	−2.6	5.3	−5.3

3a–3f indicate that the preponderance of positive lateral displacements represented load asymmetries to the left—the convex side of the scoliosis. According to the Hueter–Volkmann Law, such loading would have tended to correct the wedging asymmetry, not to increase it. Conversely, Figures 5a–5f indicate that the upper levels of the lumbar spine consistently experienced shear forces displacing the vertebrae to the left, and the lower levels experienced shear forces displacing the vertebrae to the right, thereby tending to increase the scoliosis.

In the symmetric spine, the greatest lateral offset was 4.7 mm (at L1–L2 for axial rotation efforts), and the greatest angulation of the resultant force from the axial direction was 3.8° (at L5–S1 for lateral bending effort; see Table 1). The forces acting on the motion segments were symmetric about the sagittal plane for flexion and extension efforts. For the spine geometry with scoliosis, the lateral offsets were seldom more than 5 mm different from those for the symmetric spine (see Figures 3a–f), whereas the angulation of the resultant force was several times that for the symmetric spine (Figures 5a–5f).

The maximum effort achieved and the intervertebral force magnitude declined by 9–36% with increasing scoliosis except for right axial rotation, where the maximum effort increased by 26% (Figure 7). The magnitudes of the intervertebral forces (Table 2) were reduced correspondingly.

The calculated spinal forces were dependent on the values of the motion segment stiffness and on the bounds placed on intervertebral motion. In the sensitivity study in which the analyses for the 100% scoliosis were repeated with the motion segment stiffness in all degrees of freedom reduced by a factor of two, the calculated maximum efforts were reduced by between 21% and 30%. The values obtained for the four parameters of intervertebral forces (Figs 3–6), however, correlated highly (R^2 between 0.7 and 0.97) with those from the original analyses. The values obtained for these parameters were be-

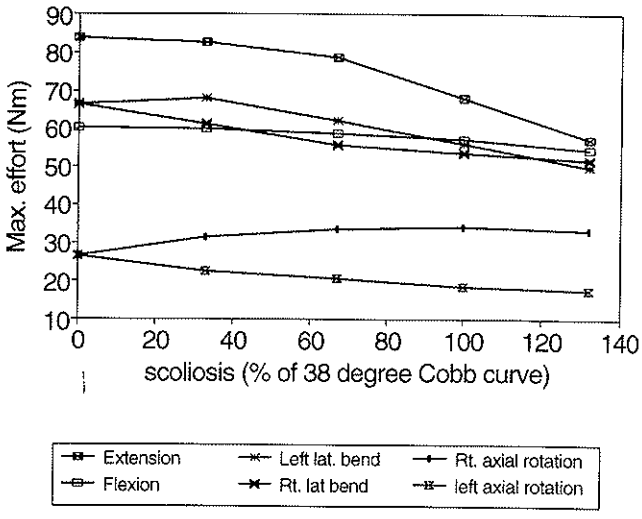

Figure 7. Maximum efforts expressed as a moment at T12 (vertical axis) plotted as a function of the degree of scoliosis (percentage of the reference scoliosis geometry, which was a 38° Cobb angle curve).

Table 2. Intervertebral Force Magnitude (N)

	Extension Effort	Flexion Effort	Left Lateral Effort	Right Lateral Effort	Right Axial Effort	Left Axial Effort
T12–L1						
0% scoliosis	1647	1028	1422	1422	1270	1262
132% scoliosis	1065	759	823	981	817	628
L1–L2						
0% scoliosis	1707	1100	1483	1483	1369	1369
132% scoliosis	1075	755	985	943	952	754
L2–L3						
0% scoliosis	1702	1213	1411	1411	1382	1382
132% scoliosis	1072	845	1034	933	1043	950
L3–L4						
0% scoliosis	1936	1206	1329	1329	1328	1328
132% scoliosis	1209	1068	1091	1098	1122	1035
L4–L5						
0% scoliosis	2148	1216	1453	1453	1412	1412
132% scoliosis	1395	1168	1336	1275	1339	1034
L5–S1						
0% scoliosis	2124	1215	1473	1473	1464	1464
132% scoliosis	1452	1149	1411	1323	1438	1019

tween 7% and 34% less, based on the slope of the regression between the values for the softened motion segments and the original values.

■ Discussion

These analyses indicate that lumbar scoliosis produces asymmetric spinal loading characterized by shear forces tending to increase the scoliosis, an axial torque tending to increase the axial plane (rotational) deformity, but little increase in the lateral offset of the resultant forces transmitted through motion segments. The overall hypotheses of this work is that mechanical forces influence growth, and hence spinal shape, in a potentially vicious cycle in growing children. If scoliosis progression results from muscle-generated asymmetric loading, it appears from the results of this study that it is the shear force component more than the lateral bending moment that is responsible for this progression. Asymmetric loading may cause progression of scoliosis by producing asymmetric growth of vertebrae and discs in young patients and asymmetric remodeling in skeletally mature patients. The findings also indicate that patients with scoliosis would be able to achieve somewhat lesser maximum efforts compared with those without scoliosis, assuming that there were no adaptive changes in the muscles to compensate for the asymmetric geometry.

For the maximum efforts analyzed here, the lateral offset of load from the disc center was as much as 9.5 mm, and the angle of the resultant force with respect to the motion segment axis was as much as 34°. The exact effect of such loading on spinal growth and curve progression is not known, because the exact sensitivity of growth and remodeling to such forces acting on the vertebrae and discs is unknown. Also, the importance of the duration of loading is unknown. It is assumed here that the spinal posture is constant and that forces associated with large voluntary efforts are more important than low level (*e.g.*, gravitational) forces applied chronically.

There was a lack of continuity of the intervertebral force offsets ϵ_y, and ϵ_x with respect to increasing scoliosis evident in Figures 3 and 4. The relations for the force angulation Θ_{ap} (Figure 5) appeared more continuous. This indicates that the solution to the linear programming problem is quite sensitive to geometric changes. Most of the discontinuities probably were due to the solution reaching a bound on muscle force or intervertebral displacement and then having to find a different strategy to circumvent this bound for the next spinal shape. It may be that the real neuromuscular control strategy, especially for submaximal efforts, would be more continuous, but it is probable that the same underlying trends (or lack of them) evident in Figures 3–7 still would be present.

The findings reported here are subject to the limitations of the simplifications and assumptions made in the analyses. They apply only to maximum efforts, but if the activation strategy of muscles were constant (all muscle forces increasing in proportion to the required effort), then the findings also would apply to submaximal efforts. It was assumed that there were no adaptive changes in the muscles, in that the maximum force that could be generated by each muscle was identical for the analyses with and without scoliosis (although the length of the muscle and the direction of the muscle forces did change). In reality, the muscles of patients with scoliosis may be subject to the physiologic length–tension effects as increasing scoliosis changes the resting length of the muscles. With time, there may be adaptive strengthening

of selected muscles leading to strength asymmetries of the muscles pairs, which was not considered in these analyses. In these static analyses, limits were placed on the amount of the intervertebral displacements based on known physiologic limits.[11] These limits placed bounds on the forces and moments in the motion segments. This, in turn, limited the degree of asymmetric loading, as is evident in, for example, Figure 3, which shows that in right lateral bending, the force lateral offsets for all levels except T12–L1 reached a limit of approximately 6 mm for the smaller Cobb angle simulations because of this effect. The results therefore are dependent on the limits placed in the analyses on the intervertebral displacements (each intervertebral lateral bending motion assumed less than 2°). A larger limit would permit greater moment transmission and hence greater lateral offset. The results of the analyses also are subject to the values chosen for the motion segment stiffness and the bounds on intervertebral motion. The sensitivity studies, however, indicated that the trends of asymmetric intervertebral loading with increasing scoliosis reported here are relatively insensitive to motion segment stiffness.

Despite these limitations, these analyses do provide insight into the loads acting on the spine in scoliosis. If quantitative information on the growth sensitivity to vertebral loading were available, then a predictive model of scoliosis progression during growth could be formulated by combining knowledge of the tissue loads with the biologic responses (growth and remodeling). Similarly, this information would permit more rational design of treatments such as braces that are intended to limit curve progression through selective modification of the forces acting on the growing spine.

Acknowledgments

The authors thank Dr. Tony Keller for providing the MRI images for reconstruction of abdominal muscle geometry.

References

1. Arkin AM, Katz JF. The effects of pressure on epiphyseal growth. The mechanism of plasticity of growing bone. J Bone Joint Surg 1956;38A:1056–76.
2. Bjerkreim I, Hassan I. Progression in untreated idiopathic scoliosis after end of growth. Acta Orthop Scand 1982;53: 897–900.
3. Gardner-Morse MG, Laible JP, Stokes IAF. Incorporation of spinal flexibility measurements into finite element analysis. J Biomechanical Eng 1990;112:481–3.
4. Han JS, Ah JY, Goel VK, Takeushi R, McGowan D. CT-based geometric data of human spine musculature. Part 1. Japanese patients with chronic low back pain. J Spinal Disord 1992;5:448–58.
5. Hueter C. Anatomische Studien an den Extremitaetengelenken Neugeborener und Erwachsener. Virkows Archiv Path Anat Physiol 1862;25:572–99.
6. Lonstein JE, Carlson JM. The prediction of curve progression in untreated idiopathic scoliosis during growth. J Bone Joint Surg [Am] 1984;66:1061–71.
7. Miller JAA, Skogland LB. Musculoskeletal interactions in the adolescent spine. Paper VI in: Skogland LB, Miller JAA, eds. On the Importance of Growth in Idiopathic Scoliosis: A Biochemical, Radiological and Biomechanical study. Oslo: Biomechanics Laboratory, University of Oslo, Norway, 1980.
8. Panjabi MM, Brand RA, White AA. Three-dimensional flexibility and stiffness properties of the human thoracic spine. J Biomech 1976;9:185–92.
9. Reuber M, Schultz A, McNeill T, Spencer D. Trunk muscle myoelectric activities in idiopathic scoliosis. Spine 1983;8:447–56.
10. Roaf R. Vertebral growth and its mechanical control. J Bone Joint Surg [Br] 1960;42:40–59.
11. Stokes IAF, Gardner-Morse M. Lumbar spine maximum efforts and muscle recruitment patterns predicted by a model with multijoint muscles and joints with stiffness. J Biomech 1995;28:173–86.
12. Stokes IAF, Aronsson DD, Urban JPG. Biomechanical factors in progression of skeletal deformities: A review. The European Journal of Experimental Muskuloskeletal Research. 1994;3:51–60.
13. Volkmann R. Verletzungen und Kankenheiten der Bewegungsorgane. In: von Pitha und Billroth, eds. Handbuch der Allgemeinen und Speciellen Chirurgie Bd II Teil II. Stuttgart: Ferdinand Enke, 1882.
14. Weinstein SL, Ponseti IV. Curve progression in idiopathic scoliosis. J Bone Joint Surg [Am] 1983;65:447–55.
15. Zetterberg C, Bjork R, Ortengren R, Andersson GB. Electromyography of the paravertebral muscles in idiopathic scoliosis: Measurements of amplitude and spectral changes under load. Acta Orthop Scand 1984;55:304–9.

Address reprints requests to

Ian A. F. Stokes
Department of Orthopaedics and Rehabilitation
Stafford Hall
University of Vermont
Burlington, VT 05405
E-mail: stokes@med.uvm.edu

Erratum

SPINE 2001;26:1638

Re: Stokes IAF. Analysis of symmetry of vertebral body loading consequent to lateral spinal curvature. Spine 1997;22(21):2495–2503:

The symbol key to the legends for Figures 4, 5, and 6 were mistakenly omitted. Each figure legend should contain the following key: ◇=T12–L1; ×=L1–2; +=L2–3; ▽=L3–4; □=L4–5; △=L5–S1.

Spine 2001 July 15;26(14):1638